

Overcoming Therapeutic Resistance in HER2-Positive Breast Cancers with CDK4/6 Inhibitors

Highlights

- Cyclin D1/CDK4 mediate resistance to HER2 blockade in HER2⁺ breast cancer
- CDK4/6 inhibition suppresses mTORC1, relieving inhibition of EGFR family kinases
- Combined CDK4/6 and HER2 inhibition is effective in transgenic and PDX mouse models
- CDK4/6 inhibitors delay tumor recurrence in a transgenic HER2⁺ breast cancer model

Authors

Shom Goel, Qi Wang, April C. Watt, ..., Eric P. Winer, Ian E. Krop, Jean J. Zhao

Correspondence

shom_goel@dfci.harvard.edu (S.G.), jean_zhao@dfci.harvard.edu (J.J.Z.)

In Brief

Goel et al. show that cyclin D1/CDK4 mediate targeted therapy resistance in HER2⁺ breast cancer. CDK4/6 inhibition overcomes this resistance by increasing tumor cell dependence on EGFR family kinase signaling. CDK4/6 inhibitors resensitize PDX tumors to HER2-targeted therapies and delay tumor recurrence *in vivo*.

Overcoming Therapeutic Resistance in HER2-Positive Breast Cancers with CDK4/6 Inhibitors

Shom Goel,^{1,*} Qi Wang,^{2,16} April C. Watt,² Sara M. Tolaney,¹ Deborah A. Dillon,³ Wei Li,^{4,5} Susanne Ramm,^{6,7} Adam C. Palmer,^{6,8,9} Haluk Yuzugullu,² Vinay Varadan,¹⁰ David Tuck,^{11,17} Lyndsay N. Harris,¹² Kwok-Kin Wong,¹ X. Shirley Liu,^{4,5} Piotr Sicinski,^{2,13} Eric P. Winer,¹ Ian E. Krop,^{1,18} and Jean J. Zhao^{2,14,15,18,*}

¹Department of Medical Oncology, Dana-Farber Cancer Institute, Boston, MA 02215, USA

²Department of Cancer Biology, Dana-Farber Cancer Institute, Boston, MA 02215, USA

³Department of Pathology, Harvard Medical School, Boston, MA 02115, USA

⁴Department of Biostatistics and Computational Biology, Dana-Farber Cancer Institute, Harvard School of Public Health, Boston, MA 02215, USA

⁵Center for Functional Epigenetics, Dana-Farber Cancer Institute, Boston, MA 02215, USA

⁶Laboratory of Systems Pharmacology, Harvard Program in Therapeutic Science, Harvard Medical School, Boston, MA 02115, USA

⁷Renal Division, Department of Medicine, Brigham and Women's Hospital, Boston, MA 02115, USA

⁸Department of Systems Biology, Harvard Medical School, Boston, MA 02115, USA

⁹School of Biotechnology and Biomolecular Sciences, University of New South Wales, Sydney, NSW 2052, Australia

¹⁰Case Comprehensive Cancer Center, Case Western Reserve University, Cleveland, OH 44106, USA

¹¹Department of Pathology, Yale University, New Haven, CT 06520, USA

¹²Case Western Reserve School of Medicine, Cleveland, OH 44106, USA

¹³Department of Genetics, Harvard Medical School, Boston, MA 02115, USA

¹⁴Department of Biological Chemistry and Molecular Pharmacology, Harvard Medical School, Boston, MA 02115, USA

¹⁵The Broad Institute of MIT and Harvard, Cambridge, MA 02142, USA

¹⁶Present address: Department of Pathology and Laboratory Medicine, Medical University of South Carolina, Charleston, SC 29425, USA

¹⁷Present address: Curis, Inc., Lexington, MA 02421, USA

¹⁸Co-senior author

*Correspondence: shom_goel@dfci.harvard.edu (S.G.), jean_zhao@dfci.harvard.edu (J.J.Z.)

<http://dx.doi.org/10.1016/j.ccr.2016.02.006>

SUMMARY

Using transgenic mouse models, cell line-based functional studies, and clinical specimens, we show that cyclin D1/CDK4 mediate resistance to targeted therapy for HER2-positive breast cancer. This is overcome using CDK4/6 inhibitors. Inhibition of CDK4/6 not only suppresses Rb phosphorylation, but also reduces TSC2 phosphorylation and thus partially attenuates mTORC1 activity. This relieves feedback inhibition of upstream EGFR family kinases, resensitizing tumors to EGFR/HER2 blockade. Consequently, dual inhibition of EGFR/HER2 and CDK4/6 invokes a more potent suppression of TSC2 phosphorylation and hence mTORC1/S6K/S6RP activity. The suppression of both Rb and S6RP enhances G1 arrest and a phenotype resembling cellular senescence. *In vivo*, CDK4/6 inhibitors sensitize patient-derived xenograft tumors to HER2-targeted therapies and delay tumor recurrence in a transgenic model of HER2-positive breast cancer.

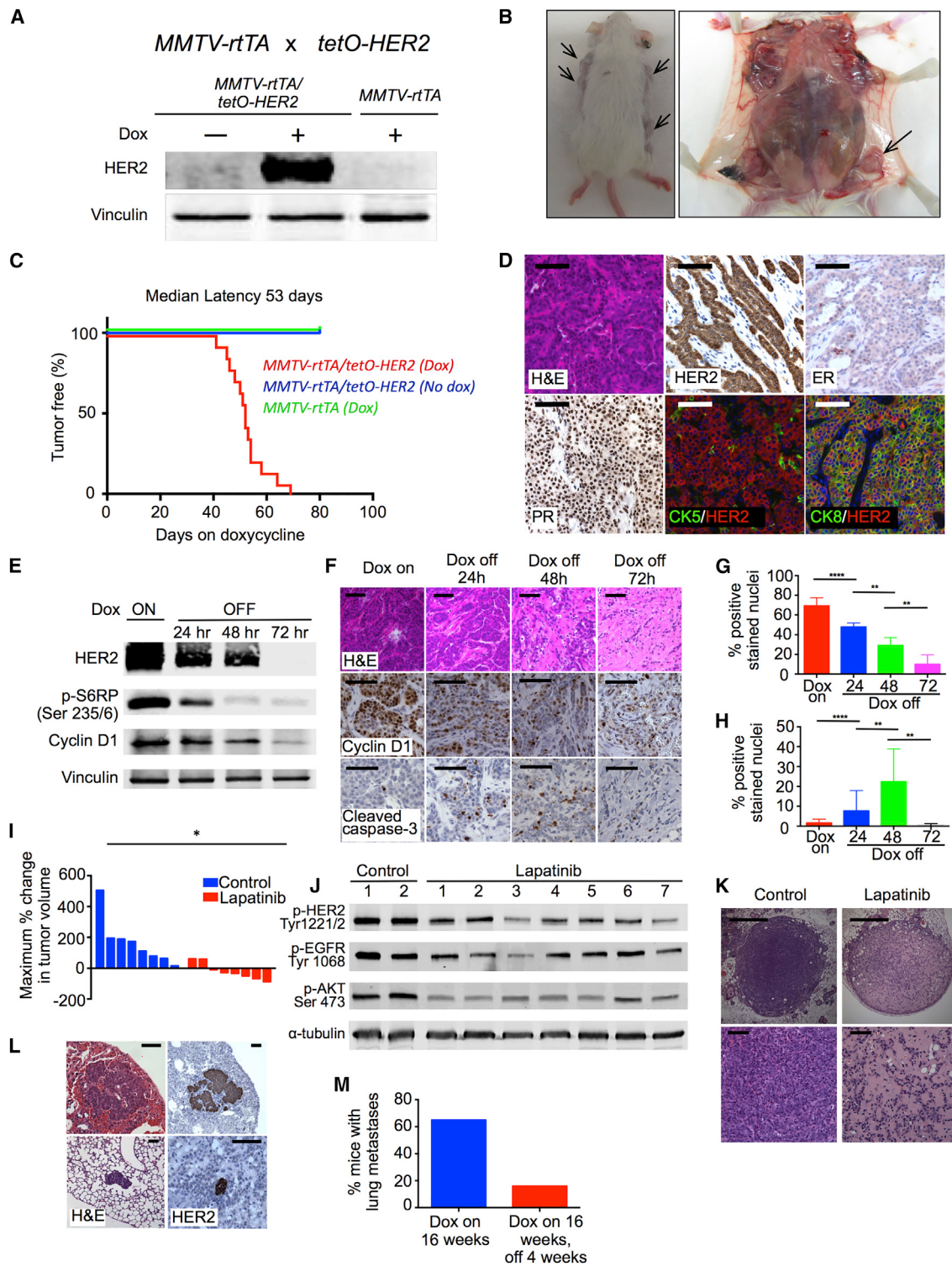
INTRODUCTION

The human epidermal growth factor receptor 2 (HER2) receptor tyrosine kinase is overexpressed in approximately 15% of human breast cancers (Slamon et al., 1987). This overexpression

is typically triggered by amplification of the wild-type *ERBB2* gene, which encodes for HER2 and serves as a bona fide oncogene (Di Fiore et al., 1987). Through dimerization with either other HER family members or itself, HER2 activates downstream signaling pathways that ultimately promote tumorigenesis,

Significance

Despite successful HER2-directed therapies, many patients with HER2-positive breast cancer will succumb to their disease once tumor cells develop resistance. Here, we show that the cyclin D1-CDK4 pathway can mediate this resistance, and that targeting resistant tumor cells with a CDK4/6 inhibitor resensitizes them to anti-HER2 therapy by increasing their dependence on EGFR family kinase signaling. Concomitant HER2 and CDK4/6 inhibition synergistically inhibits cell proliferation, controls tumor growth *in vivo*, and delays tumor recurrence in a transgenic mouse model. These effects are associated with a reduction in the phosphorylation of both Rb and S6RP, two important mediators of the G1/S transition. Our results have led to the development of a randomized clinical trial for patients with metastatic HER2-positive breast cancer.

**Figure 1. Characterization of the *MMTV-rtTA/tetO-HER2* Mouse Model**

(A) Top: Breeding scheme to create *MMTV-rtTA/tetO-HER2* mice. Bottom: 8-week-old bitransgenic mice were fed a doxycycline diet for 48 hr and mammary gland lysates were analyzed with western blots. *MMTV-rtTA* mice served as controls.

(B) Mammary tumors (arrows) in a *MMTV-rtTA/tetO-HER2* mouse after 12 weeks of doxycycline.

(C) Time to first palpable tumor in *MMTV-rtTA/tetO-HER2* mice. Doxycycline-naïve bitransgenic mice and doxycycline-treated *MMTV-rtTA* mice served as controls.

(D) Representative staining of *MMTV-rtTA/tetO-HER2* tumors.

(legend continued on next page)

cellular proliferation, survival, invasion, and metastasis (reviewed in [Arteaga and Engelman, 2014](#)).

As of 2016, four targeted therapies have been approved for the treatment of HER2-positive breast cancer: the anti-HER2 monoclonal antibodies trastuzumab and pertuzumab, the HER2/epidermal growth factor receptor (EGFR) kinase inhibitor lapatinib, and the antibody-drug conjugate trastuzumab emtansine (T-DM1) (reviewed in [Moasser and Krop, 2015](#)). Despite these advances, many patients with HER2-positive breast cancer still succumb to their disease. The main reason behind this is tumor resistance to existing therapies. Early-stage tumors that resist adjuvant therapy will relapse in distant sites, and these metastatic lesions in turn ultimately evade the effects of HER2-targeting. Therefore, understanding the mechanisms by which HER2-positive breast cancers recur and develop therapeutic resistance is critical.

A number of mechanisms have been proposed to mediate the resistance of HER2-positive breast cancers to targeted therapy. Hyperactivation of the downstream phosphoinositide 3-kinase (PI3K)-AKT pathway is the best characterized of these, and activating mutations in *PIK3CA* or loss of the lipid phosphatase PTEN each confer resistance to HER2-directed therapies in pre-clinical models ([Berns et al., 2007](#); [Nagata et al., 2004](#); [Wang et al., 2015](#)). Other proposed resistance mechanisms include alterations in the HER2 receptor, activation of parallel signaling pathways, overexpression of cyclin E, and variations in host-tumor immune interactions. Notably, correlative science from clinical trials has yet to validate any of these mechanisms (reviewed in [Moasser and Krop, 2015](#)). In this study, we sought to develop a clinically relevant transgenic mouse model of HER2-positive breast cancer that could be used to uncover mechanisms of resistance to HER2-pathway blockade. We also aimed to validate findings from this model in cell lines, patient-derived xenografts, and clinical specimens, and to translate our results into a therapeutic strategy that could be rapidly evaluated in clinical trials.

RESULTS

A Transgenic Mouse Model of HER2-Positive Breast Cancer Facilitates Genetic and Pharmacologic Simulation of HER2-Pathway Blockade

To conduct clinically relevant studies of HER2-positive breast cancer, we established a transgenic mouse model of the disease. We aimed to create mice bearing mammary carcinomas driven by wild-type human HER2, arising in a developmentally normal mammary gland and immune-competent host. To this

end, we synthesized a 4.75-kb DNA segment containing seven direct repeats of the tetracycline (tet)-operator sequence, followed by wild-type human *ERBB2* and SV40 poly(A) ([Perera et al., 2009](#)) (Figure S1A). The construct was injected into FVB/N blastocysts and the *tetO-HER2* transgenic founders were bred with *MMTV-rtTA* mice (reverse tetracycline-controlled transactivator under control of the mouse mammary tumor virus promoter), producing bitransgenic mice harboring both activator and responder transgenes (*MMTV-rtTA/tetO-HER2*) (Figure 1A).

Adult mice showed normal mammary gland architecture in the absence of doxycycline (not shown). Induction of mammary gland HER2 expression was seen within 48 hr of introducing a doxycycline-containing diet (Figure 1A). After 2 weeks of continuous HER2 induction, adult mammary ductal trees showed increased lateral branching and ductal ectasia (Figure S1B). HER2 expression within these ducts was confined to the luminal epithelium, evidenced by co-localization of HER2 and luminal marker cytokeratin 8 (CK8), but not the basal marker CK5 (Figure S1C).

Sustained HER2 induction in female bitransgenic mice (beginning at 8 weeks of age) led to the development of mammary tumors with 100% penetrance and a median latency of approximately 2 months (Figures 1B and 1C). Tumor histology was consistent with moderate to poorly differentiated adenocarcinoma admixed with foci of ductal carcinoma in situ (DCIS), thus resembling human HER2-positive breast cancers (Figure 1D). Carcinoma cells strongly overexpressed membranous HER2, showed variable staining for nuclear estrogen and progesterone receptors, and continued to co-express luminal epithelial markers (Figure 1D).

In recent years, breast cancer subclassification has extended to include assessments of gene expression, using methods such as PAM50 intrinsic subtyping ([Parker et al., 2009](#)). To assess whether the *MMTV-rtTA/tetO-HER2* tumors resembled human HER2-positive cancers on this level, we assessed tumor expression of murine orthologs of PAM50 genes and compared it with that of non-induced adult mammary glands. Tumors showed lower expression of genes in the "Luminal A" and "Normal-like" categories, and overexpressed genes in the "Luminal B," "HER2-enriched," and "Basal" categories (Figure S1D). Notably, the latter three categories collectively encompass two-thirds of human HER2-positive breast cancers and three-quarters of estrogen-receptor negative, HER2-positive breast cancers ([Carey et al., 2014](#)).

To simulate therapeutic HER2 blockade genetically, we withdrew doxycycline from *MMTV-rtTA/tetO-HER2* tumor-bearing mice, invoking a rapid decline in tumor HER2 levels (Figure 1E).

(E) Western blots on *MMTV-rtTA/tetO-HER2* tumor lysates from mice on doxycycline or after doxycycline withdrawal.

(F) Representative staining of tumors from the experiment in (E).

(G) Percentage of cyclin D1-stained nuclei in tumors from experiment depicted in (F).

(H) Percentage of cleaved caspase-3-stained nuclei in tumors from experiment depicted in (F). For (G) and (H), n = 6 per group; **p ≤ 0.01, ****p ≤ 0.0001 by one-way ANOVA (Fisher's least significant difference test).

(I) Changes in *MMTV-rtTA/tetO-HER2* tumor volume after 10 days of lapatinib treatment (*p ≤ 0.05 by Student's t test).

(J) Western blots on tumor lysates from the experiment in (I).

(K) Representative micrographs of tumors from the experiment in (I).

(L) Representative images of lung metastases in bitransgenic mice after 16 weeks of doxycycline.

(M) Frequency of microscopic lung metastases in bitransgenic mice after 16 weeks of doxycycline with or without 4 subsequent weeks of a doxycycline-free diet. All error bars represent SD. All scale bars represent 100 μm except upper panels in (K), where scale bars represent 500 μm. See also Figure S1.

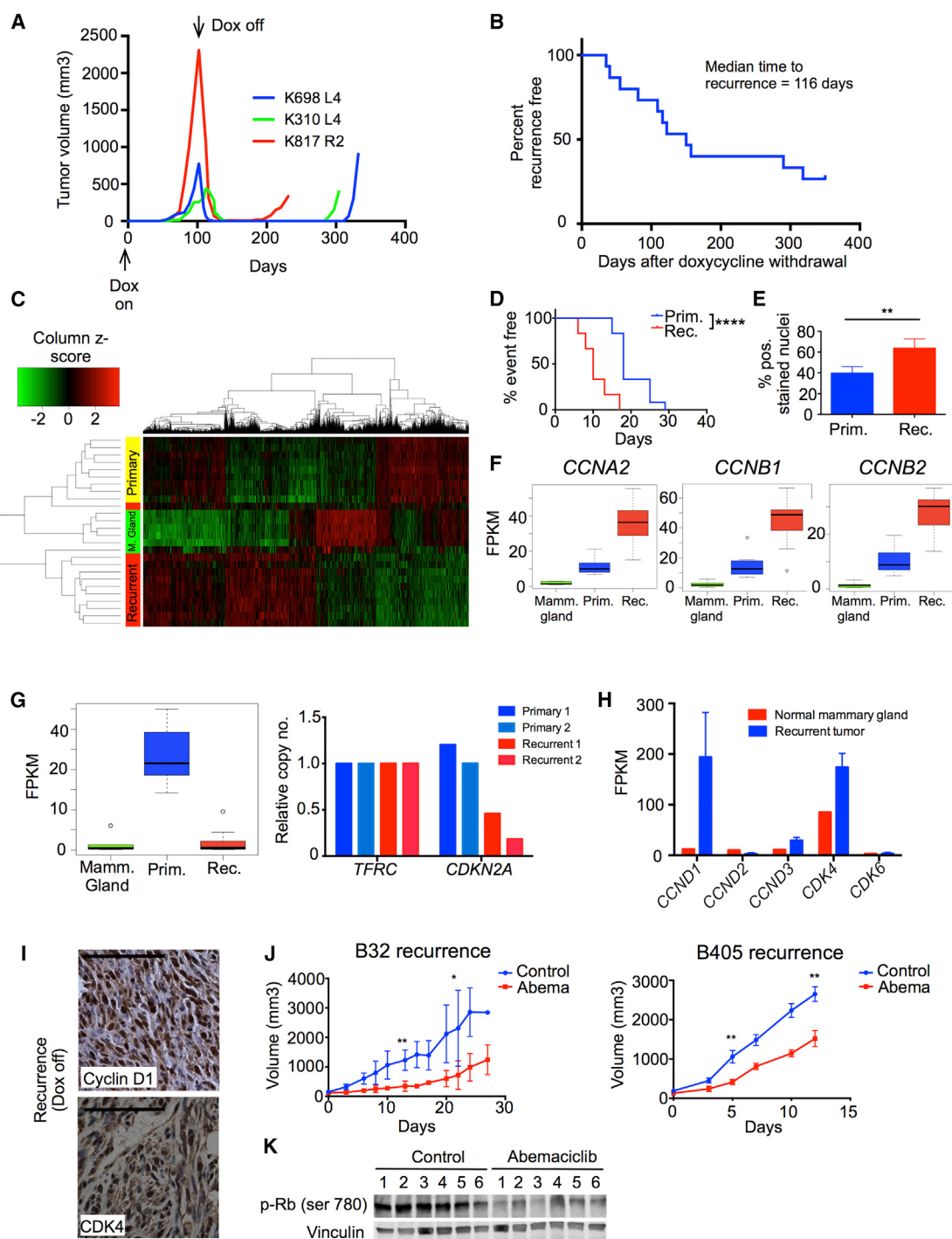


Figure 2. MMTV-rtTA/tetO-HER2 Tumors that Recur after HER2 Withdrawal Exhibit CDK4/6-Dependent Proliferation

- (A) Representative MMTV-rtTA/tetO-HER2 primary tumor growth curves during doxycycline induction and subsequent doxycycline withdrawal.
- (B) Time to development of recurrent tumors from time of doxycycline withdrawal.
- (C) Heatmap shows clustering by transcriptome-wide gene expression in normal mammary tissue ($n = 6$), primary tumors ($n = 9$), and recurrent tumors ($n = 11$) of bitransgenic mice. Columns represent genes and rows represent tumors.
- (D) Time to 5-fold increase in tumor volume for orthotopically implanted primary and recurrent tumors ($***p \leq 0.0001$ by log-rank [Mantel-Cox] test).
- (E) Percentage of Ki67-stained nuclei in primary and recurrent tumors ($n = 6$ per group). $**p \leq 0.01$ by Student's t test.
- (F) CCNA2, CCNB1, and CCNB2 transcript levels in normal mammary glands, primary tumors, and recurrent tumors.
- (G) Left: CDKN2A transcript levels in MMTV-rtTA/tetO-HER2 normal mammary glands, primary tumors, and recurrent tumors. Right: CDKN2A genomic DNA levels in primary ($n = 2$) and recurrent ($n = 2$) tumors, normalized to *TFRC* reference gene. For (F) and (G) boxes show median, 25th, and 75th percentiles, and whiskers show minimum and maximum values. FPKM, fragments per kilobase of exon per million reads mapped.
- (H) Normal mammary gland (red) vs Recurrent tumor (blue)
- (I) Immunohistochemistry for Cyclin D1 and CDK4 in recurrent tumors.
- (J) Volume (mm³) vs Days for B32 recurrence. Control (blue) vs Abema (red).
- (K) Western blot analysis for p-Rb (ser 780) and Vinculin in Control (blue) and Abemaciclib (red) treated samples.

(legend continued on next page)

This was associated with prompt deactivation of downstream signaling, including a reduction in S6-ribosomal protein (S6RP) phosphorylation (Figures 1E and S1E). The levels of cyclin D1, an essential mediator of HER2-driven mammary tumor growth that is regulated by HER2, also fell upon HER2 withdrawal (Choi et al., 2012) (Figures 1E–1G). Tumor cell apoptosis (evidenced by the presence of cleaved caspase-3) and reduced tumor cellularity were seen within 24–48 hr, followed by tumor regression within 4–5 days (Figures 1F, 1H, and S1F). Tumors typically regressed to impalpability within 3–4 weeks (Figure S1F). Pharmacologic (rather than genetic) inhibition of HER2-signaling with lapatinib also affected the growth of MMTV-*rtTA/tetO-HER2* tumors. Consistent with lapatinib's mechanism of action, treated tumors either stopped growing or regressed, and showed reduced HER2 and EGFR phosphorylation, suppression of HER2 downstream signaling, and a reduction in tumor cellularity (Figures 1I–1K and S1G–S1I).

MMTV-*rtTA/tetO-HER2* tumors also demonstrated metastatic potential, in keeping with the metastatic proclivity of human HER2-positive breast cancers. Indeed, 80% of MMTV-*rtTA/tetO-HER2* mice showed lung metastases after 16 weeks of sustained doxycycline induction (Figures 1L and 1M). Cells within these lung metastases expressed HER2 and CK8, suggesting they originated from primary mammary tumors (Figure S1J). Notably, lung metastases were seen in only 15% of mice induced for 16 weeks and subsequently maintained on a doxycycline-free diet for 4 weeks (Figure 1M), indicating ongoing HER2 dependence in metastatic lesions. Therefore, the MMTV-*rtTA/tetO-HER2* mouse model forms HER2-overexpressing mammary adenocarcinomas that resemble their human counterparts in histology, gene-expression profile, response to therapy, and metastatic potential.

Tumors Recurring after HER2 Withdrawal Exhibit Cyclin D1-CDK4-Dependent Proliferation

In patients, local and distant recurrences of breast cancer occur because a small number of tumor cells resist the effects of adjuvant therapy and later proliferate to form clinically apparent tumors. To determine whether this phenomenon could be simulated in MMTV-*rtTA/tetO-HER2* mice, we withdrew doxycycline from tumor-bearing mice and observed them for months after tumor regression. Indeed, approximately two-thirds of mice developed a recurrent mammary gland tumor ("recurrent tumors") (Figures 2A, 2B, and S2A). Non-induced mice followed for over 18 months did not develop mammary tumors, indicating that recurrent tumors were likely to be derived from cells within primary tumors rather than from unintended by-products of the mouse model (not shown). Recurrent tumors did not express the HER2 protein and thus grew by HER2-independent mechanisms (Figure S2A).

To understand how recurrent tumors differed biologically from primary tumors, we performed next-generation RNA sequencing

on a series of primary and recurrent tumors (complete data available online using NCBI Short Read Archive accession ID SRA275699). Unsupervised hierarchical clustering showed that primary and recurrent MMTV-*rtTA/tetO-HER2* tumors had distinct patterns of gene expression (Figure 2C). The expression profiles of primary and recurrent tumors differed with respect to two major groups of gene ontology terms (Figure S2B). First, recurrent tumors showed significantly downregulated expression of genes involved in the maintenance of cell membranes and cell junctions. Consistent with this and with previous reports, recurrent tumors were composed of spindle-shaped cells expressing markers indicative of an epithelial to mesenchymal transition (increase in snail, reduced β -catenin, Figure S2C) (Moody et al., 2005).

Second, recurrent tumors overexpressed genes regulating cell division and the cell cycle machinery when compared with primary tumors (Figure S2B). Given that genes within these categories could either stimulate or inhibit cell cycling, we measured the growth rate of primary and recurrent tumors to better understand this finding. We found that recurrent tumors grew more rapidly than primary tumors, and in keeping with this, recurrent tumors contained a higher fraction of Ki-67 positive cells (Figures 2D and 2E). Furthermore, recurrent tumors expressed higher levels of the mitotic phase cyclins A2, B1, and B2 and showed reduced expression of CDKN2A, which encodes the cell cycle inhibitory proteins p16 and p14^{ARF} (Figures 2F and 2G). Of note, the low CDKN2A expression was at least in part attributable to CDKN2A gene loss (Figure 2G). Collectively, these data indicate heightened activation of the cell cycle in recurrent tumors.

In HER2-positive breast cancer, cyclin D1 and its partner kinase CDK4 are critical drivers of cell proliferation. Indeed, cyclin D1 is required for the formation and maintenance of these tumors (Choi et al., 2012; Yu et al., 2001). Given the role of cyclin D1 in HER2-positive disease and robust reactivation of proliferation in recurrent tumors, we next asked whether recurrent tumor cells expressed cyclin D1, despite the lack of an upstream HER2 stimulus. Indeed, recurrent tumor cells expressed high levels of CCND1 (cyclin D1) and CDK4 transcripts when compared with normal mammary tissue (but not of CCND2, CCND3, or CDK6 transcripts) (Figure 2H), and showed strong nuclear staining for cyclin D1 and CDK4 (Figure 2I). The high CCND1 transcript levels found in recurrent tumors were not attributable to CCND1 gene amplification (Figure S2D). These findings were recapitulated in the setting of pharmacologic HER2 blockade. Upon treating a cohort of 12 MMTV-*rtTA/tetO-HER2* primary tumor-bearing mice with trastuzumab, we observed regression and subsequent regrowth in two tumors despite continued therapy. Although limited to only two cases, it is noteworthy that these trastuzumab-resistant tumors also demonstrated high levels of nuclear cyclin D1 staining (Figures S2E and S2F).

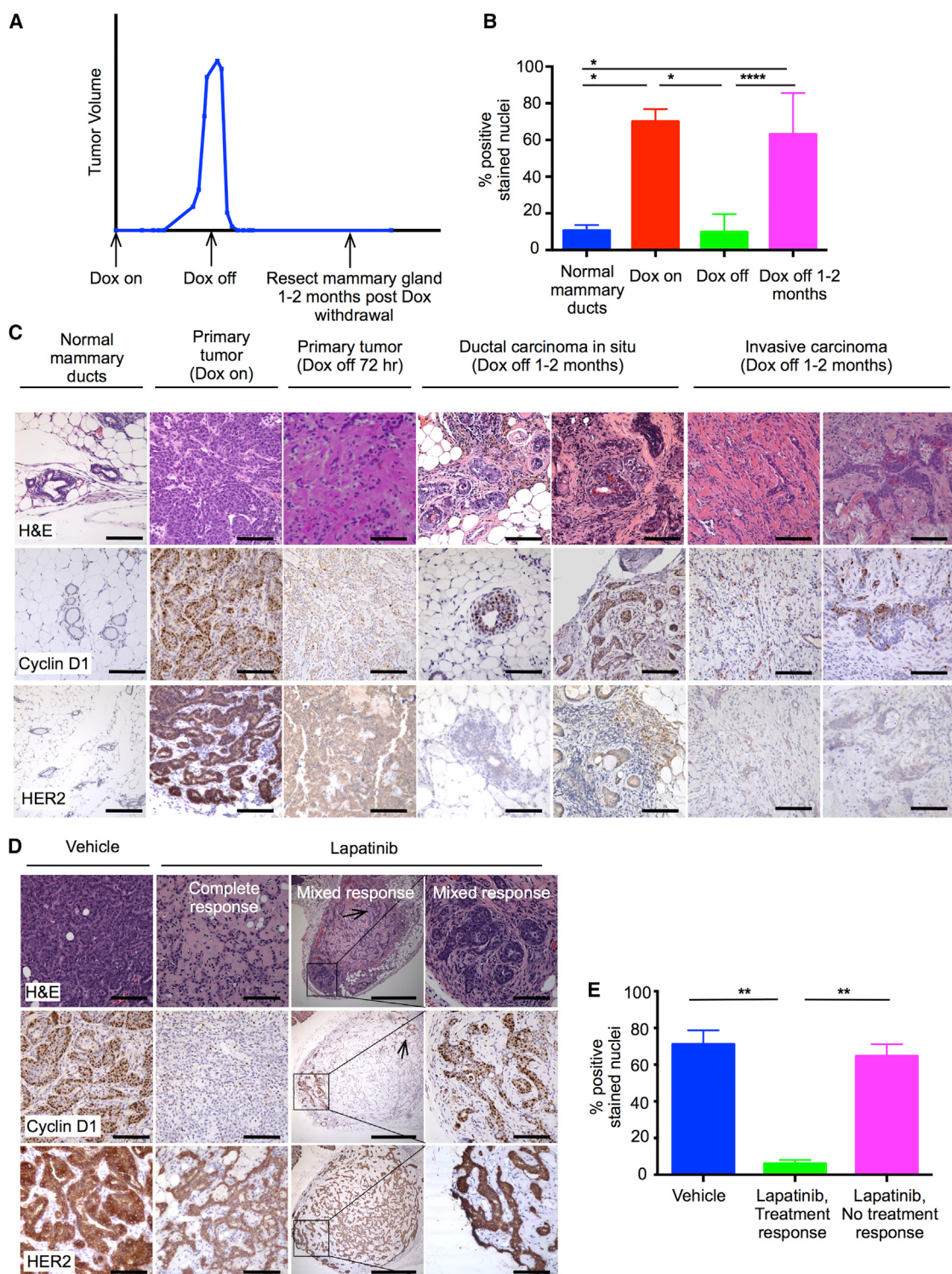
(H) CCND1, CCND2, CCND3, CDK4, and CDK6 transcript levels in MMTV-*rtTA/tetO-HER2* normal mammary glands and recurrent tumors.

(I) Representative staining of recurrent tumors for cyclin D1 and CDK4.

(J) Tumor growth in orthotopically implanted MMTV-*rtTA/tetO-HER2* recurrent tumors after treatment with abemaciclib ($n = 5$ or 6 per group). * $p \leq 0.05$, ** $p \leq 0.01$ by Student's t test.

(K) Western blot shows changes in Rb phosphorylation in B405 recurrent tumor allografts after abemaciclib treatment (5 days).

Error bars represent SD unless otherwise described. All scale bars represent 100 μm . See also Figure S2.

**Figure 3. Tumor Cells Surviving HER2-Pathway Blockade Retain Cyclin D1 Expression**

(A) Timing of mammary gland harvesting to identify residual viable tumor after HER2-withdrawal.

(B) Percentage of cyclin D1-stained nuclei in normal mammary ducts ($n = 3$), MMTV-*rtTA/tetO-HER2* primary tumors before ($n = 6$) and 72 hr after ($n = 5$) doxycycline withdrawal, and residual carcinoma cells seen 1–2 months after doxycycline withdrawal ($n = 8$) (* $p \leq 0.05$, *** $p \leq 0.0001$ by one-way ANOVA).

(C) Representative staining of tissues described in (B).

(legend continued on next page)

Intrigued by the persistence of high cyclin D1 and CDK4 levels within recurrent tumors, we next asked whether the cyclin D1-CDK4 axis was functionally important for their growth. We selected two recurrent tumors and propagated them *in vivo* in wild-type FVB mice. Treatment with a CDK4/6 inhibitor in clinical development (abemaciclib [Tate et al., 2014]) suppressed Rb phosphorylation and delayed the growth of recurrent tumors substantially (Figures 2J and 2K). Thus, although cyclin D1 levels drop abruptly in primary tumors after HER2 withdrawal (Figures 1E and 1F), recurrences arising months later retain and/or regain the expression of cyclin D1, and moreover grow in a CDK4/6-dependent manner.

In cells, cyclin D1 levels are chiefly regulated by activity of the mitogen-activated protein kinase (MAPK) pathway (which activates *CCND1* transcription) and the PI3K pathway (which regulates cyclin D1 protein stability) (Diehl et al., 1998; Sherr and Roberts, 2004). Given that recurrent tumors no longer expressed HER2, we sought to determine which pathway now played the dominant role in maintaining their high cyclin D1 level. Interestingly, mutational analysis from the RNA sequencing of primary and recurrent tumors revealed mutations in four recurrent tumors associated with hyperactivation of the MAPK pathway: two harbored hotspot mutations in KRAS (G12S and G12D) and two showed mutations in the *PTPN11* phosphatase (Figure S2G). Furthermore, cyclin D1 levels in *MMTV-rtTA/tetO-HER2* recurrent tumor-derived primary cell lines (both *KRAS* mutant and wild-type) fell to a greater extent upon treatment with an inhibitor of the MAPK pathway (MEK162) than with an inhibitor of the PI3K pathway (BKM120) (Figure S2H). Thus, the high expression of cyclin D1 in *MMTV-rtTA/tetO-HER2* tumors recurring after HER2 withdrawal is primarily driven by MAPK pathway activation.

Tumor Cells Surviving Acute HER2-Pathway Blockade

Retain Expression of Cyclin D1

We next asked whether cells that survive the initial HER2-withdrawal continue to express high levels of cyclin D1 before the development of recurrent tumors. To locate these cells, we withdrew doxycycline from *MMTV-rtTA/tetO-HER2* mice bearing primary tumors, and resected their mammary glands 1–2 months later, before tumor recurrence was seen (Figure 3A). In most cases, these mammary glands showed fibrotic tumor beds without viable tumor, suggesting near total tumor cell death after HER2 withdrawal (Figure S3A). In approximately 10% of mammary glands, however, we detected residual tumor cells either forming foci of DCIS (malignant cells within ductal lumens, surrounded by p63-expressing myoepithelial cells) or regions of invasive carcinoma (nests and cords of malignant cells without myoepithelium) (Figures 3C and S3B). These cells did not express HER2, in keeping with a sustained de-induction of the HER2 transgene (Figure 3C). Strikingly, the majority of these cells showed strong nuclear expression of cyclin D1 (Figures 3B and 3C), as well as of CDK4 and the *CDKN2A* gene product p16 (Figures S3C and S3D). Thus, although the vast majority of *MMTV-*

rtTA/tetO-HER2 cells die after HER2 withdrawal, the small surviving fraction expresses nuclear cyclin D1 weeks after HER2 withdrawal, in the absence of a HER2 stimulus.

We obtained similar results after treating a cohort of *MMTV-rtTA/tetO-HER2* tumors with lapatinib while under continuous HER2 induction. In most cases, lapatinib induced widespread cell death (Figures 1I, 1K, and 3D). However, in some cases small foci of *in situ* and/or invasive carcinoma persisted despite lapatinib treatment (Figure 3D), and again the viable tumor cells showed strong nuclear cyclin D1 expression (Figures 3D and 3E). Thus, whether HER2 signaling was blocked genetically or pharmacologically, we found an association between persistent cyclin D1 expression and sustained tumor cell viability.

The Cyclin D1-CDK4 Axis Confers Resistance to HER2-Pathway Blockade

Given our findings, we hypothesized that the cyclin D1-CDK4 axis might mediate resistance to HER2-directed therapies in HER2-positive breast cancer. To explore this further, we next treated six HER2-positive human breast cancer cell lines with lapatinib and measured changes in *CCND1* gene expression. In the three lapatinib-sensitive cell lines (BT474, ZR 75-30, SKBR3) *CCND1* mRNA levels fell acutely. In contrast, three lapatinib-resistant lines (MDA-MB-361, MDA-MB-453, UACC-732) showed little or no reduction in *CCND1* transcription (Figure 4A). Consistent with this, we found that in both BT474 and SKBR3, lapatinib strongly suppressed signaling downstream of HER2 (including p-AKT and p-S6RP) and markedly reduced cyclin D1 protein levels. Conversely, while lapatinib suppressed AKT phosphorylation in MDA-MB-453 and MDA-MB-361, the reduction in S6RP phosphorylation was limited and cyclin D1 protein levels did not change (Figure 4B). Rb phosphorylation (a marker of cyclin D1-CDK4/6 activity) was also only reduced in sensitive cell lines. Thus we observed the same association between insensitivity to HER2-pathway blockade and sustained cyclin D1 expression *in vitro* as was seen in *MMTV-rtTA/tetO-HER2* mice.

To examine whether an increased cyclin D1 level confers resistance to HER2-pathway blockade in tumor cells, we stably over-expressed *CCND1* in trastuzumab/lapatinib-sensitive breast cancer cell lines (BT474 and SKBR3) (Figure S4A), and found that this reduced sensitivity to both lapatinib and trastuzumab (Figure 4C). Conversely, knockdown of *CCND1* in resistant cells (MDA-MB-361 and MDA-MB-453) with an inducible small hairpin RNA (shRNA) (*tet-shCCND1*) (Figure S4B) partially restored the sensitivity of these cells to trastuzumab (reduced trastuzumab IC₅₀) (Figure 4D). Collectively, these results show that cyclin D1 functionally mediates (at least in part) resistance to HER2-directed agents among HER2-positive breast cancer cells.

Importantly, we observed a similar association in patients. We analyzed *CCND1* gene copy number in a cohort of HER2-positive breast cancers (n = 62) from a clinical trial of neoadjuvant chemotherapy plus trastuzumab (trial identifier NCT00148668), and observed a significant association between higher absolute

(D) Representative staining of *MMTV-rtTA/tetO-HER2* primary tumors treated with control or lapatinib. Box indicates viable DCIS, arrows indicate viable invasive carcinoma.

(E) Percentage of cyclin D1-stained nuclei in *MMTV-rtTA/tetO-HER2* primary tumor regions showing histologic response to lapatinib (n = 6), no response to lapatinib (n = 6), or after control treatment (n = 6) (**p ≤ 0.01 by one-way ANOVA).

All error bars represent SD. All scale bars represent 100 μm except third column in (D) where scale bars represent 500 μm. See also Figure S3.

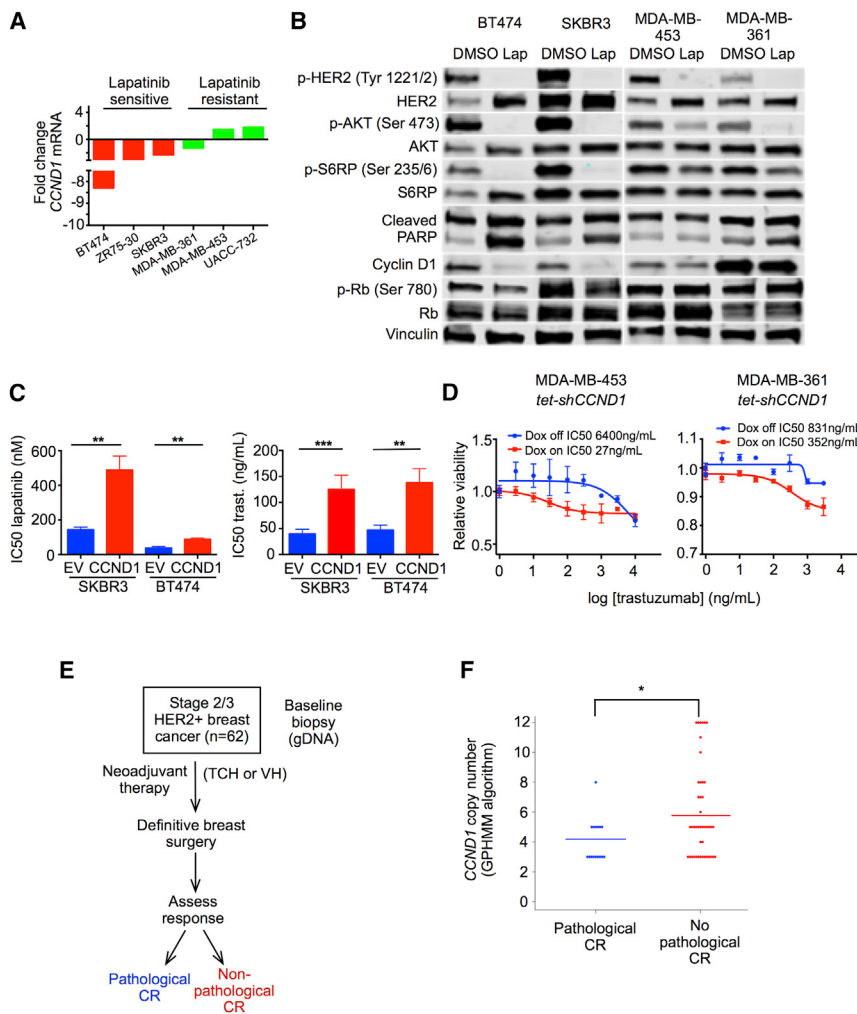


Figure 4. The Cyclin D1-CDK4 Axis Mediates Resistance to HER2-Targeted Therapy

(A) Fold change in *CCND1* gene expression in cell lines after treatment with 500 nM lapatinib for 6 hr.

(B) Western blots on cell lysates after treatment with 500 nM lapatinib or DMSO for 24 hr (note: for cleaved PARP blots, upper band represents total PARP and lower band represents cleaved PARP).

(C) Sensitivity to lapatinib or trastuzumab (IC_{50}) of SKBR3/BT474 cells constitutively overexpressing *CCND1* or empty vector (EV). ** $p \leq 0.01$, *** $p \leq 0.001$ by one-way ANOVA.

(D) Relative viability of MDA-MB-453 *tet-shCCND1* and MDA-MB-361 *tet-shCCND1* cells in response to trastuzumab in the presence or absence of doxycycline.

(E) Design of clinical trial NCT00148668 (TCH: docetaxel, carboplatin, trastuzumab; VH: vinorelbine, trastuzumab).

(F) *CCND1* copy number (determined by a Global Parameter Hidden Markov Model) by pathological complete response status in the NCT00148668 trial. Each dot represents an individual patient and lines represent means (* $p = 0.016$ by Wilcoxon signed rank test).

All error bars represent SD. See also Figure S4.

CCND1 copy number in HER2-positive breast cancers and the failure to achieve a pathological complete response to treatment (Figures 4E and 4F). It is unclear whether this finding implies a purely prognostic or also a predictive role for *CCND1* gene amplification, as all subjects received chemotherapy plus trastuzumab. Nonetheless, an association between cyclin D1 amplification and a worse response to a trastuzumab-containing regimen was seen.

Combined HER2-CDK4/6 Inhibition Synergistically Suppresses Tumor Cell Proliferation

Having found that genetic knockdown of *CCND1* increased the sensitivity of HER2-resistant cells to trastuzumab, we next investigated how pharmacologic inhibition of the cyclin D1/CDK4 axis would affect sensitivity to HER2-directed therapies. We first used cells isolated directly from *MMTV-rtTA/tetO-HER2* primary tumors and cultured them in doxycycline to maintain HER2 expression. Although both lapatinib and trastuzumab had some growth-inhibitory effect on *MMTV-rtTA/tetO-HER2* cells, the addition of the CDK4/6 inhibitor abemaciclib to either agent significantly enhanced this (Figure S5A).

We next treated three lapatinib-resistant HER2-positive breast cancer cell lines (MDA-MB-453, MDA-MB-361, UACC-732) with

a wide range of lapatinib/abemaciclib concentration pairings in a combinatorial matrix experiment, as shown in Figure S5B. For each of the three cell lines, we observed single-agent activity of the CDK4/6 inhibitor abemaciclib, but more remarkably a potent synergistic inhibition of cell viability after combined treatment (combination indices of 0.23, 0.13, and 0.4 respectively, where a combination index <1 implies synergy) (Chou and Talalay, 1984) (Figures 5A, S5B, and S5C). Therefore, CDK4/6 inhibition restores the sensitivity of resistant tumor cells to the effects of HER2 inhibitors. We repeated these experiments in lapatinib-sensitive cell lines (BT474 and SKBR3), and also observed a synergistic interaction between lapatinib and abemaciclib, but to a lesser degree (combination indices 0.49 and 0.56) (Figures S5D–S5F).

In clinical practice, patients often demonstrate initial sensitivity to HER2-directed therapies and subsequently develop resistance. We therefore tested whether CDK4/6 inhibition could also restore therapeutic sensitivity in cell lines with acquired (rather than de novo) resistance. To this end, we tested the effect of abemaciclib on previously described derivatives of BT474 and SKBR3 cells that had acquired resistance to trastuzumab after prolonged culture in trastuzumab (Konecny et al., 2006). In both cases, trastuzumab had little effect on cell viability, as expected. However, although abemaciclib showed some activity, the abemaciclib/trastuzumab combination had a greater effect than abemaciclib alone, again suggesting that inhibition of CDK4/6 restores sensitivity to anti-HER2 therapies (Figure 5B). Furthermore, HER2-positive cell lines conditioned to develop resistance to the HER2-directed antibody-drug conjugate trastuzumab emtansine (T-DM1) also retained sensitivity

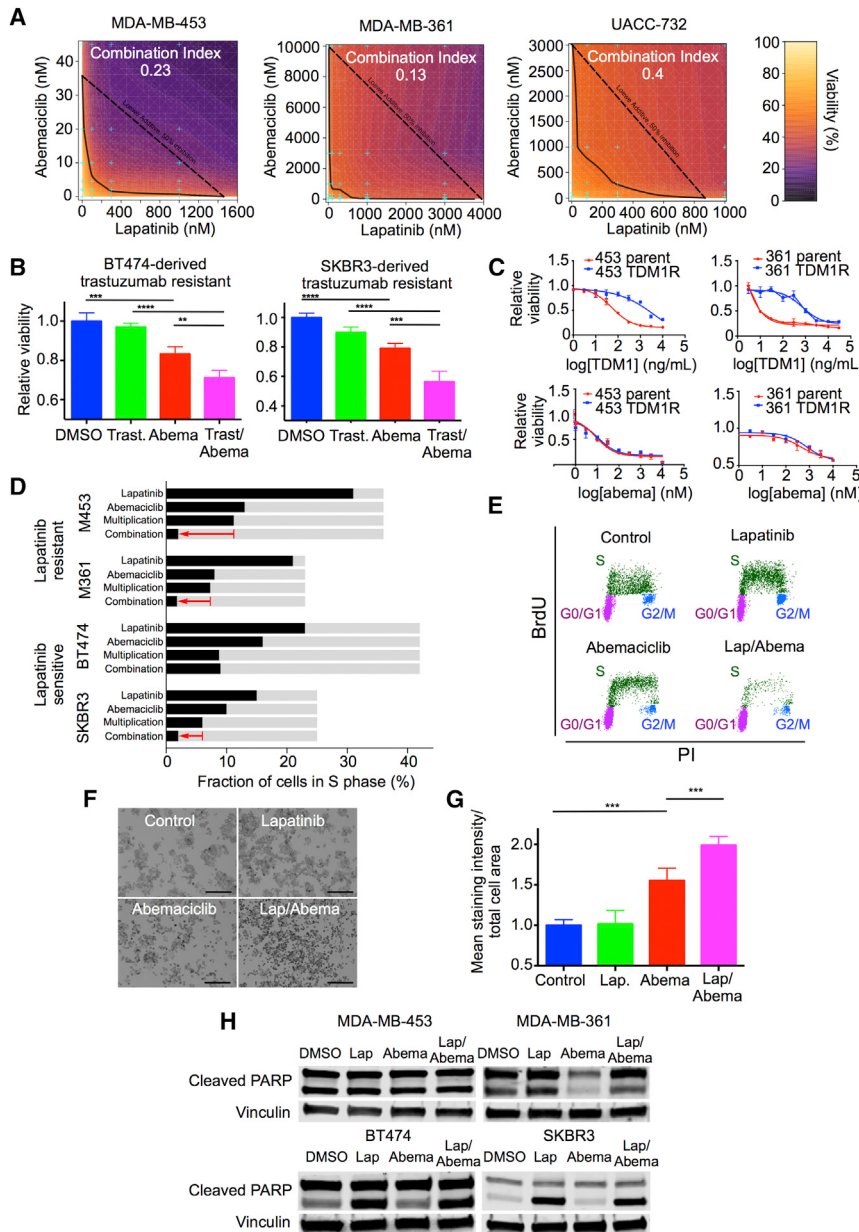


Figure 5. The Effects of Combined CDK4/6-HER2 Inhibition on Cellular Viability, Proliferation, and Apoptosis

(A) Isobolograms showing actual (heatmap, and solid line at 50% inhibition) and predicted additive (dashed line) effects of combined abemaciclib/lapatinib therapy on viability of MDA-MB-453, MDA-MB-361, and UACC-732 cells.

(B) Viability of trastuzumab-resistant SKBR3 and BT474 cells after treatment with 300 ng/ml trastuzumab and/or 300 nM abemaciclib.

(C) Top: Viability of parental or T-DM1-resistant MDA-MB-361 or MD-MB-453 cells after T-DM1 treatment. Bottom: Viability of the same cells after abemaciclib treatment.

(D) Effect of lapatinib and/or abemaciclib on percentage of cells in S phase. Light gray bars indicate control values. “Multiplication” shows expected effect of combined treatment if single-agent effects were multiplied; red arrow indicates actual effect of combination. MDA-MB-361/MDA-MB-453: 100 nM lapatinib, 25 nM abemaciclib. BT474: 25 nM lapatinib, 75 nM abemaciclib. SKBR3: 25 nM lapatinib, 500 nM abemaciclib. 48 hr treatment.

(E) Representative flow cytometry plots of MDA-MB-453 cells (from experiments in D) labeled with anti-bromodeoxyuridine and propidium iodide.

(F) Representative SA- β -galactosidase staining in MDA-MB-453 cells treated with lapatinib (100 nM) and/or abemaciclib (25 nM). Stained cells appear dark (black and white photographs).

(G) Mean staining intensity for cells in (F).

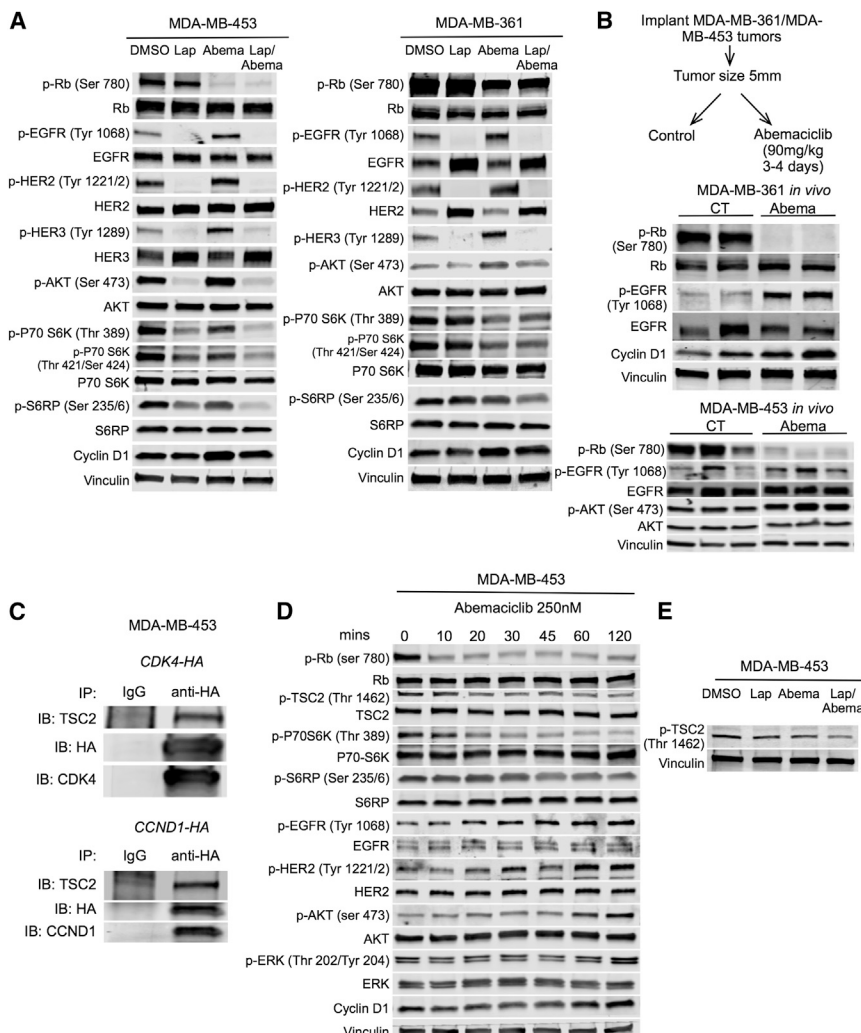
(H) Cleaved PARP levels after treating cells with DMSO, lapatinib, and/or abemaciclib. BT474 and SKBR3: 100 nM lapatinib, 300 nM abemaciclib; MDA-MB-361: 500 nM lapatinib, 300 nM abemaciclib; MDA-MB-453: 500 nM lapatinib, 25 nM abemaciclib. (Note: for cleaved PARP blots, upper band represents total PARP and lower band cleaved PARP.)

All error bars represent SD. **p ≤ 0.01, ***p ≤ 0.001, ****p ≤ 0.0001 by one-way ANOVA. See also Figure S5.

to abemaciclib (Figure 5C). Thus, CDK4/6 inhibition may remain an effective strategy in the face of resistance to cytotoxins.

The synergistic effect on cell viability seen with combined CDK4/6 and HER2 inhibition could be mediated by changes in proliferation, apoptosis, or both. To explore this, we first assessed the effects of anti-HER2 or combination treatment on cell cycle progression. In *MMTV-rtTA/tetO-HER2* tumor-derived primary cells, the combination of HER2 and CDK4/6 inhibition produced the greatest reduction in the percentage of cells in S phase (Figure S5G). Similar results were seen in HER2-positive human cell lines: in lapatinib-resistant cells (MDA-MB-453 and MDA-MB-361), lapatinib had very little impact on the percentage of cells in S phase. However, combined lapatinib/abemaciclib treatment resulted in a significantly greater degree of cell cycle

arrest than abemaciclib alone (Figures 5D, S5H, and S5I). Scatterplots showed a pronounced G1 arrest in these cells (Figure 5E). Indeed, the effect of lapatinib and abemaciclib combined was even stronger than would be expected if the individual effects of the two agents were multiplied (Bliss, 1939) (Figure 5D). In lapatinib-sensitive cell lines (BT474 and SKBR3), the lapatinib/abemaciclib combination substantially reduced the percentage of cells in S phase, in one cell line matching the multiplicative expectation and in the other cell line slightly exceeding that which would be expected if mono-therapy effects were multiplied (Figures 5D, S5J, and S5K). Previously, cell cycle arrest in solid tumors after cyclin D1 ablation has been associated with development of a phenotype resembling cellular senescence (Choi et al., 2012). Consistent



with this, we observed an increase in senescence-associated β -galactosidase expression in MDA-MB-453 cells treated with abemaciclib. Notably, combined lapatinib/abemaciclib treatment increased this even further (Figures 5F and 5G).

We also sought evidence of increased tumor cell apoptosis in response to combination treatment. For each of four cell lines, we administered drugs at concentrations that had yielded synergistic effects on cell viability in previous experiments and had induced at least a 70% reduction in viability. In no cell line did the addition of abemaciclib to lapatinib increase poly(ADP) ribose polymerase (PARP) cleavage when compared with lapatinib monotherapy (Figure 5H). Thus the enhanced inhibition of cell viability seen upon combining CDK4/6 and HER2 inhibitors (when compared with either agent alone) appears to be mediated by increased suppression of cellular proliferation rather than heightened apoptosis.

CDK4/6 Inhibition Reduces mTORC1 Activity, and Is Associated with Increased Activity of EGFR Family Kinases

Given the synergy observed with the lapatinib/abemaciclib combination, we next examined whether CDK4/6 inhibition alters ac-

Figure 6. Effects of CDK4/6 Inhibition on Signal Transduction in Treatment-Resistant HER2-Positive Breast Cancers

(A) MDA-MB-453 and MDA-MB-361 cells were treated with lapatinib and/or abemaciclib for 24 hr and cell lysates were probed with the antibodies shown (concentrations as in Figure 5H).

(B) MDA-MB-361 and MDA-MB-453 xenografts were treated with control or abemaciclib for 3–4 days. Tumor lysates were probed with the antibodies shown.

(C) Anti-HA immunoprecipitates from CCND1-HA or CDK4-HA transfected MDA-MB-453 cells were immunoblotted for TSC2.

(D) MDA-MB-453 cells were treated with abemaciclib and cell lysates were probed with the antibodies shown.

(E) MDA-MB-453 cells were treated as in (A) and cell lysates probed with the antibodies shown. See also Figure S6.

tivity of lapatinib targets (EGFR family kinases). We treated MDA-MB-453 and MDA-MB-361 cells with lapatinib, abemaciclib, or their combination, specifically selecting drug concentrations that had shown synergy in combinatorial therapy experiments (Figure 5A) and induced at least 70% inhibition of cell viability (e.g. 25 nM abemaciclib for MDA-MB-453 and 300 nM abemaciclib for MDA-MB-361). Strikingly, abemaciclib treatment increased phosphorylation of EGFR family kinases (EGFR, HER2, and HER3) in both cell lines (Figure 6A). Furthermore, AKT phosphorylation increased in both lines, consistent with increased signaling

through these receptor tyrosine kinases (Figure 6A). Similar changes were observed *in vivo* when lapatinib-resistant xenografts were treated with abemaciclib (Figure 6B).

Interestingly, although abemaciclib increased EGFR family and AKT phosphorylation, this was not accompanied by an increase in markers of downstream mTOR signaling. Rather, phosphorylation of P70-S6 kinase and S6RP at known activation sites was somewhat reduced (Figure 6A). These changes began rapidly after abemaciclib exposure, suggesting that they are mediated by acute changes in protein phosphorylation (Figures S6A and S6B). Notably, reduced P70-S6K activity is known to relieve feedback inhibition on EGFR family kinase signaling, and the triad of reduced P70-S6K activity, increased RTK/AKT phosphorylation, and unchanged levels of total RTK protein is suggestive of an inhibitory stimulus at the level of mTORC1 (Chandraratna et al., 2011).

We therefore next sought to determine how CDK4/6 inhibitors might suppress mTORC1 activity and thus relieve feedback inhibition on RTKs. After considering various canonical regulators of mTORC1, we focused on the protein TSC2 (tuberin), which lies directly upstream of mTORC1. Phosphorylation of TSC2 at particular sites enhances mTORC1 and thus P70-S6K activity

(Inoki et al., 2002), and the cyclin D1/CDK4 complex has previously been shown to directly interact with TSC2 and regulate its phosphorylation in human osteosarcoma cells (Zacharek et al., 2005).

We first confirmed an interaction between TSC2 and members of the cyclin D1/CDK4 complex: CDK4 was overexpressed in MDA-MB-453 cells by transfection of an HA-tagged *CDK4* construct. Immunoprecipitation with an anti-HA antibody pulled down TSC2 (Figure 6C). We also found that TSC2 was pulled down using the same technique in *CCND1-HA*-transfected cells (Figure 6C). To determine whether CDK4 could also regulate TSC2 phosphorylation, we suppressed CDK4 expression in MDA-MB-453 cells with an inducible shRNA and found reduced TSC2 phosphorylation at Thr 1462 (Figure S6C). In addition, pharmacologic CDK4/6 inhibition with abemaciclib reduced TSC2 phosphorylation in several HER2-positive breast cancer cell lines (Figures 6D, 6E, and S6D).

The abemaciclib-induced reduction in TSC2 phosphorylation was seen within 10 min of abemaciclib treatment, accompanied by a reduction in downstream P70-S6K and S6RP phosphorylation (Figure 6D), validating prior reports that the cyclin D1/CDK4 complex regulates TSC2 phosphorylation (Zacharek et al., 2005). The associated increase in RTK and AKT/ERK phosphorylation was observed shortly after this (EGFR at 20–30 min, HER2 and 30–60 min, and AKT/ERK at 60–120 min in MDA-MB-453 cells). This temporal sequence shows that a CDK4/6 inhibitor-induced reduction in mTORC1 activity (associated with reduced phosphorylation of TSC2) precedes the increased phosphorylation of upstream RTKs (Figure 6D).

Combined CDK4/6-HER2 Inhibition Increases Suppression of mTORC1 Activity

We next focused on changes in intracellular signaling that are unique to combination therapy, which might underlie the synergistic effects on cell proliferation. Given that Rb phosphorylation is a critical determinant of cell cycle progression into S phase and that combined lapatinib/abemaciclib increased cell cycle arrest in G1 (Figures 5D and 5E), we explored whether combination treatment is associated with an even greater reduction in Rb phosphorylation than that seen after abemaciclib monotherapy. However, we did not observe a difference in Rb phosphorylation between cells treated with combination treatment or abemaciclib alone, suggesting that the augmentation of cell cycle arrest after combination treatment was not due to increased suppression of Rb phosphorylation (Figure 6A). Strikingly, however, TSC2, P70-S6K, and S6RP phosphorylation were most heavily suppressed in cells treated with combination therapy (Figures 6A and 6E).

We next sought corroborating molecular evidence to support these observations. We observed similar changes in the phosphorylation of EGFR, HER2, HER3, and AKT (increased) as well as P70-S6K and S6RP (decreased) in MDA-MB-453 cells using genetic knockdown of *CDK4* or *CCND1* instead of abemaciclib, suggesting that our findings were directly related to inhibition of the cyclin D1/CDK4 axis rather than due to an “off-target” effect of abemaciclib (Figures S6E and S6F). Conversely, overexpression of *CCND1* in the lapatinib-sensitive cell line BT474 (which reduced lapatinib sensitivity, Figure 4E) led to reductions in EGFR, HER2, and AKT phos-

phorylation and an increase in P70-S6K phosphorylation (Figure S6G).

The Effects of Combined CDK4/6 and HER2 Inhibition *In Vivo*

We next explored the effects of combined CDK4/6 and HER2 inhibition *in vivo*. We utilized five mouse models of HER2-positive breast cancer in total and treated tumor-bearing mice with anti-HER2 therapies (trastuzumab or lapatinib), abemaciclib, their combination, or control. Of note, for long-term studies of tumor growth, we chose trastuzumab as the anti-HER2 therapy because lapatinib and abemaciclib have overlapping gastrointestinal toxicities, rendering the lapatinib/abemaciclib combination an unlikely candidate for future clinical development.

For *MMTV-rtTA/tetO-HER2* primary tumors, trastuzumab monotherapy induced a non-significant inhibition in tumor growth, abemaciclib monotherapy significantly delayed tumor growth, and the combination delayed tumor growth more than either single agent (Figures 7A and 7B). In BT474 xenografts, both trastuzumab and abemaciclib monotherapies slowed tumor growth but did not induce regression. *In vivo*, combination therapy induced tumor regressions, and in some cases no viable tumor was seen in the mammary gland at the completion of therapy (Figure 7C).

We next studied the effects of combination trastuzumab/abemaciclib in two patient-derived xenograft (PDX) models of HER2-positive treatment-refractory breast cancer. The first was derived from a heavily pretreated patient’s liver metastasis (PDX 14-07, ER-positive, Figure 7D) and the second from brain metastatic tissue (PDX BT-355, ER-negative, Figure S7A). At the time of tissue biopsy to create these models, the patients’ tumors had already developed resistance to several prior lines of systemic therapy (as shown). In keeping with the trastuzumab-refractory nature of these tumors, we observed no effect of trastuzumab on xenograft growth. Abemaciclib slowed tumor growth without inducing regressions. Strikingly, the abemaciclib/trastuzumab combination resulted in either tumor regression (PDX 14-07) or a significantly greater growth delay (PDX BT-355) (Figures 7D and S7A).

Consistent with our *in vitro* findings, we also noted that short-term treatment of MDA-MB-453 xenografts with the lapatinib/abemaciclib combination resulted in the greatest suppression of proliferation, with little effect on apoptosis (Figures 7E and S7B). Furthermore, β -galactosidase expression was also highest in dual-treated MDA-MB-453 xenografts (Figure 7F). Collectively these data add further support to the notion that combination CDK4/6-HER2 inhibition acts primarily through enhancement of G1 arrest, associated with cellular senescence.

CDK4/6 Inhibition Delays the Recurrence of HER2-Driven Breast Cancers *In Vivo*

Given our findings that (1) cells surviving HER2 blockade continue to express cyclin D1 and CDK4, (2) recurrent tumors grow in a CDK4/6-dependent fashion, and (3) combined HER2-CDK4/6 inhibition acts synergistically against HER2-therapy resistant cells, we next performed experiments to determine whether early CDK4/6 inhibition could delay the onset of recurrence in the *MMTV-rtTA/tetO-HER2* mouse model.

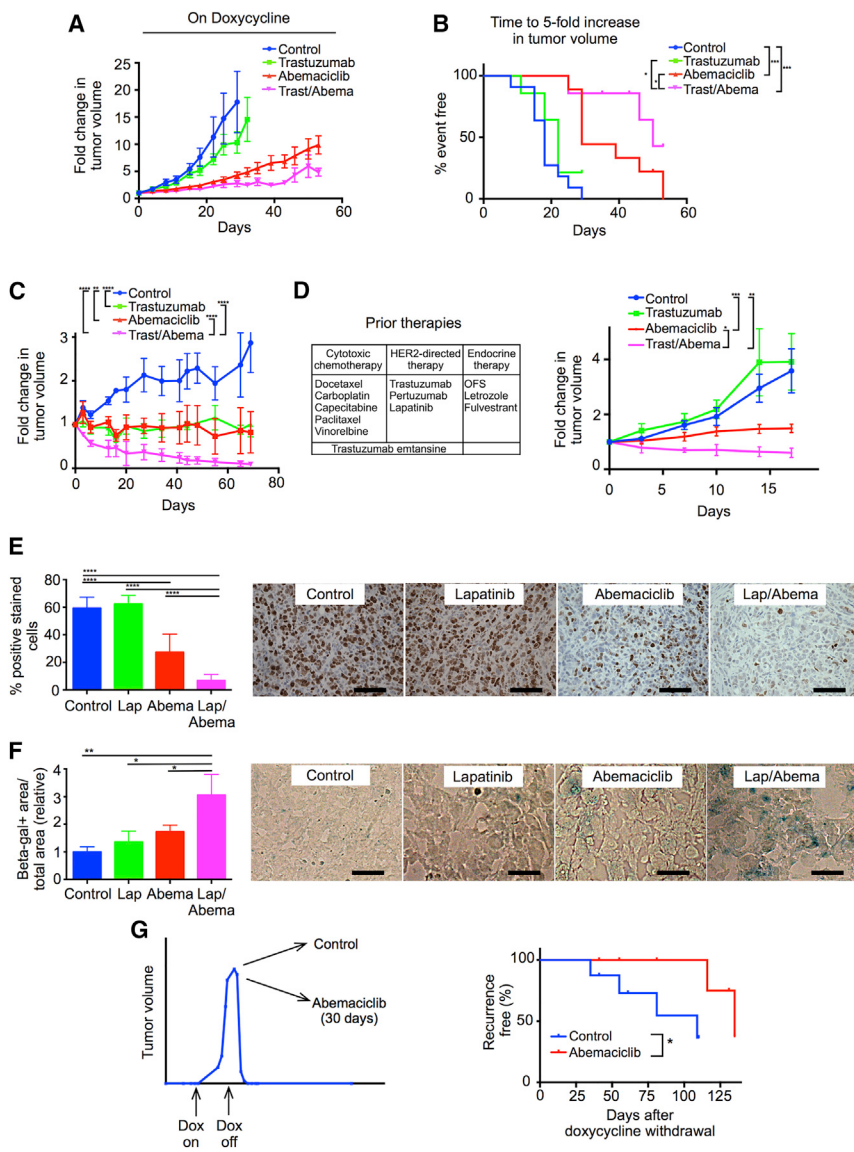


Figure 7. The Effects of Combined CDK4/6-HER2 Inhibition In Vivo

(A) Growth curves for *MMTV-rtTA/tetO-HER2* primary tumors treated with control, trastuzumab, and/or abemaciclib.

(B) Time to 5-fold increase in tumor volume (analysis by log-rank [Mantel-Cox] test) from the experiment in (A).

(C) BT474 tumor growth after treatment with control, trastuzumab, and/or abemaciclib.

(D) Tumor growth of PDX model 14-07 (patient's prior treatments shown; OFS, ovarian function suppression) after treatment with control, trastuzumab, and/or abemaciclib. Analysis in (C) and (D) by one-way ANOVA (Kruskal-Wallis test).

(E) Percentage of Ki-67-positive cells in MDA-MB-453 xenografts after 5 days of treatment with lapatinib and/or abemaciclib, with representative micrographs.

(F) Relative β -galactosidase positive area/total area in MDA-MB-453 xenografts after 5-day treatment with lapatinib and/or abemaciclib, with representative micrographs.

(G) Time to development of recurrent tumors after doxycycline withdrawal in *MMTV-rtTA/tetO-HER2* mice treated with abemaciclib versus control for 30 days at time of doxycycline withdrawal.

Data shown to maximum follow-up of 135 days (analysis by log-rank [Mantel-Cox] test). * $p \leq 0.05$, ** $p \leq 0.01$, *** $p \leq 0.001$, **** $p \leq 0.0001$. Data analysis was by one-way ANOVA unless otherwise indicated. All error bars represent SD. All scale bars represent 100 μ m. See also Figure S7.

(3) an intact immune system is present; and (4) HER2 expression is mammary-specific and inducible. The inducibility is important because it allows for mammary gland development under normal physiological conditions. Indeed, constitutive overexpression of HER2 during mammary development alters mammary duct structure, and it is not known how the biology of

tumors forming within such developmentally abnormal glands is altered (Mukherjee et al., 2000).

Our results using the mouse model, cell line assays, xenografts, and clinical specimens indicate that: (1) the survival of cells after HER2-pathway blockade is associated with retained expression of cyclin D1; (2) cyclin D1 and CDK4 mediate resistance to HER2-targeted therapies; and (3) CDK4/6 inhibitors can overcome this resistance by resensitizing tumors to HER2-directed therapies. The latter point is underscored by the synergy observed with combined HER2-CDK4/6 inhibition *in vitro* and *in vivo*.

We provide both pharmacologic and genetic data to suggest possible mechanisms behind this synergy. We show that in HER2-therapy-resistant tumors, suppression of CDK4 activity reduces TSC2 phosphorylation at Thr1462. As would be expected, this is associated with a partial suppression of mTORC1 and, hence, P70-S6K activity. We suggest that this reduction in P70-S6K activity then relieves feedback inhibition of upstream EGFR family kinases. These data are consistent with previous

We induced HER2-positive tumor formation in a cohort of *MMTV-rtTA/tetO-HER2* mice, and once tumors reached 15 mm in size we withdrew doxycycline. At that time, mice were randomly assigned to begin treatment with abemaciclib or control vehicle for 30 days and were monitored for the development of recurrent disease. The onset of recurrent disease was significantly prolonged in abemaciclib-treated mice (median time to recurrence 108 versus 135 days, hazard ratio 0.23, $p = 0.035$) (Figure 7G).

DISCUSSION

We first set out to explore mechanisms of resistance to HER2-directed therapies by creating a transgenic mouse model of HER2-positive breast cancer. It is worth noting that the *MMTV-rtTA/tetO-HER2* mouse model is unique in that it satisfies several criteria: (1) tumors are driven by wild-type HER2 (mimicking the human disease); (2) tumors express human HER2, facilitating studies with therapeutic human-specific anti-HER2 antibodies;

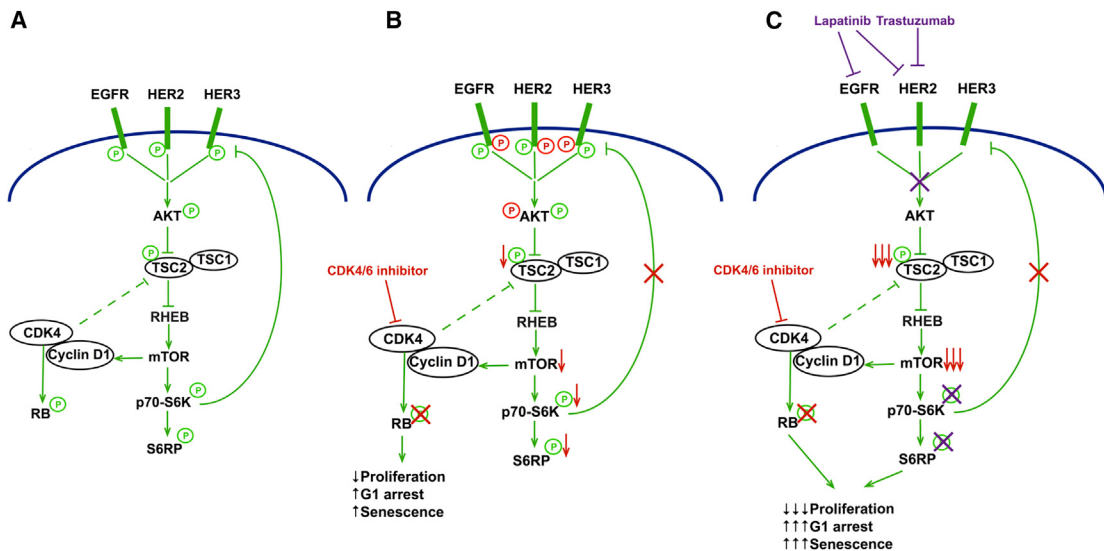


Figure 8. CDK4 Inhibition Resensitizes HER2-Therapy-Resistant Tumors to Inhibition of EGFR Family Kinases

(A) Under basal conditions, signaling downstream of EGFR family kinases stimulates both P70-S6K (via AKT/mTOR) and Rb phosphorylation (via cyclin D1/CDK4). S6K exerts negative feedback to partially suppress the RTK signaling. In addition, cyclin D1/CDK4 bind to and regulate TSC2, further enhancing mTOR activity. (B) After CDK4/6 inhibitor treatment (changes in red), Rb phosphorylation is potentially suppressed inducing a partial G1 arrest. CDK4/6 inhibition also leads to a reduction in TSC2 phosphorylation, resulting in partial suppression of mTOR and, thus, S6K activity. The suppression of S6K activity relieves feedback inhibition on EGFR family kinases, evidenced by increased EGFR family and AKT phosphorylation. (C) When CDK4/6 inhibitor treated cells are co-treated with anti-HER2 therapy, synergy is observed. First, the increased EGFR/HER2 activity “primes” cells to the effects of anti-HER2 therapy (in purple). Second, when both CDK4/6 and HER2 are inhibited, there is maximal suppression of TSC2 phosphorylation. Together, these induce a more complete shutdown of S6RP phosphorylation. Thus, combined therapy inhibits both Rb and S6RP phosphorylation, further reducing cellular proliferation.

reports showing that the cyclin D1/CDK4 complex interacts with TSC2 and regulates its phosphorylation (Zacharek et al., 2005), and that reduced P70-S6 kinase activity relieves feedback inhibition of EGFR family kinases (Chandarlapaty et al., 2011). We have not shown here that CDK4 directly phosphorylates TSC2 at Thr1462, and deeper exploration of the cyclin D1-CDK4/TSC2 interaction and of other mechanisms by which CDK4/6 inhibitors might regulate mTORC1 is ongoing.

Based on our data, synergy between CDK4/6 and HER2 inhibitors has two potential origins: (1) most directly, both CDK4/6 and EGFR/HER2 (via AKT) trigger TSC2 phosphorylation, and their dual inhibition induces a more marked suppression of p-TSC2 and hence mTORC1 activity; (2) indirectly, the CDK4/6 inhibitor-induced reduction of TSC2 phosphorylation attenuates mTORC1 activity, relieving feedback inhibition of EGFR family kinases, in turn rendering cells more sensitive to the effects of EGFR/HER2 inhibitors. Collectively, these two phenomena lead to a more potent suppression of S6RP phosphorylation with combination treatment (Figure 8).

Our *in vitro* and *in vivo* data reveal that combined HER2-CDK4/6 inhibition does not increase tumor cell apoptosis. Rather, cells and xenografts exposed to combination therapy show reduced cellular proliferation characterized by G1 arrest. This observation is consistent with landmark studies showing that both Rb and P70-S6K/S6RP are critical mediators of the G1/S transition (Goodrich et al., 1991; Lane et al., 1993). We also observed that the enhanced G1 arrest is associated with a heightened cellular senescence phenotype. What is not yet clear is why suppression of cell proliferation ultimately results in tumor

regressions in certain HER2-resistant xenograft models. Possibilities worth investigating include the eventual clearance of senescent cells by the immune system, or the eventual onset of apoptosis after cells are held in G1 for prolonged periods.

In combination therapy experiments, we observed consistent differences between cell lines that are resistant or sensitive to HER2-directed therapy. For example, combination indices indicating synergistic activity of dual HER2-CDK4/6 inhibition were lower in resistant cells (implying greater synergy). We speculate that this is because in sensitive cells, lapatinib alone reduces phosphorylation of both Rb and S6RP, already suppressing these two important gatekeepers of passage through G1. In these cells, adding a CDK4/6 inhibitor can somewhat enhance antitumor effects by reducing phosphorylation of one or both of these proteins slightly further. In resistant cells, lapatinib had little effect on p-Rb or p-S6RP, and abemaciclib only reduced p-Rb. Indeed in these cells only combination treatment potently suppressed both p-Rb and p-S6RP. Therefore, the effects of combination treatment are greatest in resistant cells.

Our findings also facilitate a deeper understanding of the recent literature. Resistance to PI3K pathway blockade in PIK3CA mutant breast cancer has been attributed to a persistence of mTORC1 and CDK4/6 activity, which can be overcome by inhibitors of mTOR and CDK4/6, respectively (Elkabets et al., 2013; Vora et al., 2014). We speculate that this resistance might be underscored by a persistence of TSC2 phosphorylation mediated by AKT-independent, CDK4-dependent factors.

Our data have led to the development of a randomized trial of abemaciclib in patients with advanced HER2-positive disease.

We have opted to use a trastuzumab-abemaciclib combination for the trial, exploiting the benefits of combination therapy while avoiding the overlapping toxicities of lapatinib and abemaciclib. Encouragingly, our unpublished clinical experience suggests that abemaciclib is active against HER2-therapy-resistant breast cancers, and supports the notion that these tumors can retain dependency upon CDK4/6 (Tolaney et al., 2015).

Finally, we note that our HER2 de-induction experiments in the MMTV-*rtTA/tetO-HER2* mouse mimic neoadjuvant therapy in the clinic. In HER2-positive disease, it is well established that the complete eradication of microscopic tumor during neoadjuvant therapy is strongly associated with a reduced risk of disease recurrence. Our observations that a small number of cyclin D1-expressing tumor cells survive HER2 withdrawal, and that targeting these cells with a CDK4/6 inhibitor can prolong the time to tumor recurrence, are intriguing. These results invite speculation regarding the role of CDK4/6 inhibitors as an adjuvant therapy for breast cancer, treating microscopic residual disease with a view to preventing disease recurrence.

EXPERIMENTAL PROCEDURES

Animal Experiments

Generation of *tetO-HER2* mice was performed as described in [Supplemental Experimental Procedures](#). All xenograft studies were performed in nude mice except for MDA-MB-453, which was engrafted in NSG mice. Mice were euthanized using CO₂ inhalation, and we performed all mouse experiments in accordance with protocols approved by the Institutional Animal Care and Use Committees of Dana-Farber Cancer Institute and Harvard Medical School.

RNA Sequencing

RNA isolated from mouse mammary glands and tumors was subject to quality control using the Qubit (Life Technologies) and the Bioanalyzer (Agilent). RNA was converted into a DNA library using the Ultra RNA Library Prep Kit for Illumina (New England BioLabs). After further quality control, libraries were sequenced on the HiSeq 2000 (Illumina).

Patients

Patients were enrolled in a clinical trial (NCT00148668) of trastuzumab plus either vinorelbine or docetaxel/carboplatin as neoadjuvant therapy for stage 2/3 HER2-positive breast cancer. *CCND1* copy number was determined using previously described methods (Li et al., 2011). The protocol was approved by Institutional Review Boards of all participating sites (Dana-Farber, Brigham and Women's Hospital, Massachusetts General Hospital, Beth Israel Deaconess Hospital, Yale University). All patients provided informed consent to participate.

Statistical Analysis

Statistical analysis was performed as described for each experiment. Repeated-measures one-way ANOVA was used for the analysis of primary tumor growth curves. Survival analysis was performed using the log-rank (Mantel-Cox) test. All statistical tests were two-sided. Differences were considered statistically significant at a p value of less than 0.05.

ACCESSION NUMBERS

The accession number for the RNA-sequencing reported in this paper is NCBI Short Read Archive: SRA275699.

SUPPLEMENTAL INFORMATION

Supplemental Information includes Supplemental Experimental Procedures and seven figures and can be found with this article online at <http://dx.doi.org/10.1016/j.ccr.2016.02.006>.

AUTHOR CONTRIBUTIONS

Conceptualization, S.G., J.J.Z.; Methodology, S.G., Q.W., D.T., J.J.Z.; Verification, S.G., A.C.W.; Formal Analysis, S.G., W.L., S.R., A.C.P., V.V., X.S.L.; Investigation, S.G., A.C.W., Q.W., S.M.T., H.Y., D.A.D., L.N.H; Resources, K.K.W., X.S.L., E.P.W., I.E.K., J.J.Z.; Data Curation, S.G., W.L.; Writing – Original Draft, S.G.; Writing – Review & Editing, S.G., P.S., S.M.T., I.E.K., J.J.Z.; Supervision, E.P.W., I.E.K., J.J.Z.; Funding Acquisition, E.P.W., I.E.K., J.J.Z.

ACKNOWLEDGMENTS

A.C.W. and Q.W. contributed equally to this work. We thank Dr Roderick Bronson from the Rodent Histopathology Core Facility at Harvard Medical School (HMS) for helpful discussions regarding mouse pathology, and Dr Peter Sorger from the Department of Systems Biology at HMS for his advice and support. We also thank Mayuko Segawa for technical assistance. We thank Neil O'Brien (UCLA) for the gift of trastuzumab-resistant BT474 and SKBR3 cell lines. This study was supported by NIH P50 CA168504 (to E.P.W.) and CA172461 (to J.J.Z.), a Susan G. Komen grant SAC 10005 (to I.E.K.), the Breast Cancer Research Foundation (to E.P.W. and J.J.Z.), and Aid for Cancer Research (to E.P.W.). Q.W. is supported by the Institutional Research Grant of Hollings Cancer Center and the Medical University of South Carolina. W.L. and X.S.L. are supported by NIH grant U01CA180980. A.C.P. is supported by the National Health and Medical Research Council of Australia. P.S. is supported by NIH grants R01 CA083688 and P01 CA080111. S.G. conducts research sponsored by Eli Lilly. S.T. receives research funding from Genentech. K.K.W. conducts research sponsored by AstraZeneca, Acetylon, and Gilead Pharmaceuticals, performs consultancy for G1 Therapeutics and Array Therapeutics, and is a founder and equity holder of G1 Therapeutics. P.S. receives research funding and serves as a consultant for Novartis.

Received: July 14, 2015

Revised: October 22, 2015

Accepted: February 9, 2016

Published: March 14, 2016

REFERENCES

- Arteaga, C.L., and Engelman, J.A. (2014). ERBB receptors: from oncogene discovery to basic science to mechanism-based cancer therapeutics. *Cancer Cell* 25, 282–303.
- Berns, K., Horlings, H.M., Hennessy, B.T., Madiredjo, M., Hijmans, E.M., Beelen, K., Linn, S.C., Gonzalez-Angulo, A.M., Stemke-Hale, K., Hauptmann, M., et al. (2007). A functional genetic approach identifies the PI3K pathway as a major determinant of trastuzumab resistance in breast cancer. *Cancer Cell* 12, 395–402.
- Bliss, C.I. (1939). The toxicity of poisons applied jointly. *Ann. Appl. Biol.* 26, 585–615.
- Carey, L.A., Barry, W.T., Pitcher, B., Hoadley, K.A., Cheang, M.C., Anders, C.K., Henry, N.L., Tolaney, S.M., Dang, C.T., Krop, I.E., et al. (2014). Gene expression signatures in pre- and post-therapy (Rx) specimens from CALGB 40601 (Alliance), a neoadjuvant phase III trial of weekly paclitaxel and trastuzumab with or without lapatinib for HER2-positive breast cancer (BrCa). *J. Clin. Oncol.* 32, 506.
- Chandrarapthy, S., Sawai, A., Scaltriti, M., Rodrik-Outmezguine, V., Grbovic-Huezo, O., Serra, V., Majumder, P.K., Baselga, J., and Rosen, N. (2011). AKT inhibition relieves feedback suppression of receptor tyrosine kinase expression and activity. *Cancer Cell* 19, 58–71.
- Choi, Y.J., Li, X., Hydbring, P., Sanda, T., Stefano, J., Christie, A.L., Signoretti, S., Look, A.T., Kung, A.L., von Boehmer, H., and Sicinski, P. (2012). The requirement for cyclin D function in tumor maintenance. *Cancer Cell* 22, 438–451.
- Chou, T.C., and Talalay, P. (1984). Quantitative analysis of dose-effect relationships: the combined effects of multiple drugs or enzyme inhibitors. *Adv. Enzyme Regul.* 22, 27–55.

- Di Fiore, P.P., Pierce, J.H., Kraus, M.H., Segatto, O., King, C.R., and Aaronson, S.A. (1987). erbB-2 is a potent oncogene when overexpressed in NIH/3T3 cells. *Science* 237, 178–182.
- Diehl, J.A., Cheng, M., Roussel, M.F., and Sherr, C.J. (1998). Glycogen synthase kinase-3beta regulates cyclin D1 proteolysis and subcellular localization. *Genes Development* 12, 3499–3511.
- Elkabets, M., Vora, S., Juric, D., Morse, N., Mino-Kenudson, M., Muranen, T., Tao, J., Campos, A.B., Rodon, J., Ibrahim, Y.H., et al. (2013). mTORC1 inhibition is required for sensitivity to PI3K p110alpha inhibitors in PIK3CA-mutant breast cancer. *Sci. Translational Med.* 5, 196ra199.
- Goodrich, D.W., Wang, N.P., Qian, Y.W., Lee, E.Y., and Lee, W.H. (1991). The retinoblastoma gene product regulates progression through the G1 phase of the cell cycle. *Cell* 67, 293–302.
- Inoki, K., Li, Y., Zhu, T., Wu, J., and Guan, K.L. (2002). TSC2 is phosphorylated and inhibited by Akt and suppresses mTOR signalling. *Nat. Cell Biol.* 4, 648–657.
- Konecny, G.E., Pegram, M.D., Venkatesan, N., Finn, R., Yang, G., Rahmeh, M., Untch, M., Rusnak, D.W., Spehar, G., Mullin, R.J., et al. (2006). Activity of the dual kinase inhibitor lapatinib (GW572016) against HER-2-overexpressing and trastuzumab-treated breast cancer cells. *Cancer Res.* 66, 1630–1639.
- Lane, H.A., Fernandez, A., Lamb, N.J., and Thomas, G. (1993). p70s6k function is essential for G1 progression. *Nature* 363, 170–172.
- Li, A., Liu, Z., Lezon-Geyda, K., Sarkar, S., Lannin, D., Schulz, V., Krop, I., Winer, E., Harris, L., and Tuck, D. (2011). GPHMM: an integrated hidden Markov model for identification of copy number alteration and loss of heterozygosity in complex tumor samples using whole genome SNP arrays. *Nucleic Acids Res.* 39, 4928–4941.
- Moasser, M.M., and Krop, I.E. (2015). The evolving landscape of HER2 targeting in breast cancer. *JAMA Oncol.* 1, 1154–1161.
- Moody, S.E., Perez, D., Pan, T.C., Sarkisian, C.J., Portocarrero, C.P., Sterner, C.J., Notorfrancesco, K.L., Cardiff, R.D., and Chodosh, L.A. (2005). The transcriptional repressor Snail promotes mammary tumor recurrence. *Cancer Cell* 8, 197–209.
- Mukherjee, S., Louie, S.G., Campbell, M., Esserman, L., and Shyamala, G. (2000). Ductal growth is impeded in mammary glands of C-neu transgenic mice. *Oncogene* 19, 5982–5987.
- Nagata, Y., Lan, K.H., Zhou, X., Tan, M., Esteva, F.J., Sahin, A.A., Klos, K.S., Li, P., Monia, B.P., Nguyen, N.T., et al. (2004). PTEN activation contributes to tumor inhibition by trastuzumab, and loss of PTEN predicts trastuzumab resistance in patients. *Cancer Cell* 6, 117–127.
- Parker, J.S., Mullins, M., Cheang, M.C., Leung, S., Voduc, D., Vickery, T., Davies, S., Fauron, C., He, X., Hu, Z., et al. (2009). Supervised risk predictor of breast cancer based on intrinsic subtypes. *J. Clin. Oncol.* 27, 1160–1167.
- Perera, S.A., Li, D., Shimamura, T., Raso, M.G., Ji, H., Chen, L., Borgman, C.L., Zaghloul, S., Brandstetter, K.A., Kubo, S., et al. (2009). HER2YVMA drives rapid development of adenosquamous lung tumors in mice that are sensitive to BIBW2992 and rapamycin combination therapy. *Proc. Natl. Acad. Sci. USA* 106, 474–479.
- Sherr, C.J., and Roberts, J.M. (2004). Living with or without cyclins and cyclin-dependent kinases. *Genes Development* 18, 2699–2711.
- Slamon, D.J., Clark, G.M., Wong, S.G., Levin, W.J., Ullrich, A., and McGuire, W.L. (1987). Human breast cancer: correlation of relapse and survival with amplification of the HER-2/neu oncogene. *Science* 235, 177–182.
- Tate, S.C., Cai, S., Ajamie, R.T., Burke, T., Beckmann, R.P., Chan, E.M., De Dios, A., Wishart, G.N., Gelbert, L.M., and Cronier, D.M. (2014). Semi-mechanistic pharmacokinetic/pharmacodynamic modeling of the antitumor activity of LY2835219, a new cyclin-dependent kinase 4/6 inhibitor, in mice bearing human tumor xenografts. *Clin. Cancer Res.* 20, 3763–3774.
- Tolaney, S.M., Rosen, L.S., Beeram, M., Goldman, J.W., Gandhi, L., Tolcher, A.W., Papadopoulos, K.P., Rasco, D.W., Myrand, S.P., Hulanthavil, P., et al. (2015). Clinical activity of abemaciclib, an oral cell cycle inhibitor, in metastatic breast cancer. *Cancer Res.* 75, P5-19-13.
- Vora, S.R., Juric, D., Kim, N., Mino-Kenudson, M., Huynh, T., Costa, C., Lockerman, E.L., Pollack, S.F., Liu, M., Li, X., et al. (2014). CDK 4/6 inhibitors sensitize PIK3CA mutant breast cancer to PI3K inhibitors. *Cancer Cell* 26, 136–149.
- Wang, Q., Liu, P., Spangle, J.M., Von, T., Roberts, T.M., Lin, N.U., Krop, I.E., Winer, E.P., and Zhao, J.J. (2015). PI3K-p110alpha mediates resistance to HER2-targeted therapy in HER2+, PTEN-deficient breast cancers. *Oncogene*. <http://dx.doi.org/10.1038/onc.2015.406>.
- Yu, Q., Geng, Y., and Sicinski, P. (2001). Specific protection against breast cancers by cyclin D1 ablation. *Nature* 411, 1017–1021.
- Zacharek, S.J., Xiong, Y., and Shumway, S.D. (2005). Negative regulation of TSC1-TSC2 by mammalian D-type cyclins. *Cancer Res.* 65, 11354–11360.